Original Article

Cytogenet Genome Res 121:88–95 (2008)
DOI: 10.1159/000125833

Cytogenetic and Genome Research

Impairment of gastric acid secretion and increase of embryonic lethality in *Foxq1*-deficient mice

W. Goering[a] I.M. Adham[a] B. Pasche[a] J. Männer[b] M. Ochs[c] W. Engel[a] B. Zoll[a]

[a]Institute of Human Genetics, and [b]Department of Anatomy and Embryology, University of Göttingen, Göttingen (Germany); [c]Institute of Anatomy, University of Bern, Bern (Switzerland)

Accepted in revised form for publication by M. Schmid, 18 January 2008.

Abstract. The mouse *Foxq1* gene, also known as *Hfh1*, encodes a winged helix/forkhead transcription factor. In adult mice, *Foxq1* is highly expressed in kidney and stomach. Here, we report that *Foxq1* is expressed during prenatal and postnatal stomach development and the transcripts are restricted to acid secreting parietal cells. Mice homozygous for a deletion of the *Foxq1* locus on a 129/Sv × C57BL/6J hybrid genetic background display variable phenotypes consistent with requirement of the gene during embryogenesis. Approximately 50% of *Foxq1*$^{-/-}$ embryos die in utero. Surviving homozygous mutants are normal and fertile, and have a silky shiny coat. Although the parietal cell development is not affected in the absence of *Foxq1*, there is a lack of gastric acid secretion in response to various secretagogue stimuli. Ultrastructural analysis suggests that the gastric acid secretion defect in *Foxq1*-deficient mice might be due to impairment in the fusion of cytoplasmic tubulovesicles to the apical membrane of secretory canaliculi.

Gastric acid secretion is required for normal digestion and nutrient absorption in human as well as for the sterilization of fluids and the prevention of bacterial overgrowth (Champagne, 1989). Gastric acid is secreted from parietal cells, which is one of the most abundant cell types in the corpus and antrum of the stomach. Histamine, gastrin and acetylcholine are the major physiological stimuli of acid secretion, which is mediated via binding of these ligands to their receptors located in the basolateral plasma membrane of parietal cells (Fukushima et al., 1999). Activation of the receptors results in initial elevation of intracellular Ca^{2+} and/or cAMP levels followed by activation of a cAMP-dependent kinase cascade that regulates membrane trafficking (Chew, 1985). Parietal cells contain abundant intracellular membrane compartments, known as tubulovesicles that contain H^+,K^+-ATPase proton pumps, located inside the tubulovesicular membrane. Upon stimulation, the tubulovesicles fuse with the apical membrane to form the extended secretory canaliculus. Exposition of the H^+,K^+-ATPase to the gastric lumen enables gastric acid secretion (Urushidani and Forte, 1997).

The mammalian forkhead box (FOX) family of transcription factors is divided into subclasses of proteins that share high homology in the winged helix DNA binding domain (Clark et al., 1993; Kaestner et al., 2000). Members of this evolutionarily conserved family are known to regulate cell fate, proliferation and tissue-specific expression in different organisms (Kaufmann and Knochel, 1996). We have characterized a member of a new subfamily of *Fox* genes, *Foxq1*, and found that *Foxq1* is highly expressed in kidney and stomach (Frank and Zoll, 1998). In vitro studies showed that *Foxq1* represses telokin promoter activity when overexpressed in the A10 vascular smooth muscle cells (Hoggatt et

This work was supported by a grant from the German Research Foundation (graduation collage 242).

W.G and I.M.A. contributed equally to this study.

Request reprints from Wolfgang Engel
Institute for Human Genetics, University of Göttingen
Heinrich-Düker-Weg 12, DE–37073 Göttingen (Germany)
telephone: +49 551 397589; fax: +49 551 399303
e-mail: wengel@gwdg.de

1424–8581/08/1212–0088$24.50/0

Accessible online at:
www.karger.com/cgr

al., 2000). The role of FOXQ1 for mammalian hair follicle development was revealed by the study of satin mutant mice (*sa*), in which a mutation in the *Foxq1* gene has been found (Hong et al., 2001). These mice have a silky shiny coat-appearance, attributable to aberrant differentiation of the hair shaft. However, a role of FOXQ1 in development and function of stomach and kidney has not been reported.

Here, we show that the specific expression of *Foxq1* in stomach is restricted to parietal cells. To address the function of *Foxq1*, we used homologue recombination in ES cells to delete the protein-coding region of the gene. On a 129/Sv × C57BL/6J hybrid genetic background, 50% of the homozygous null embryos die in utero. Surviving *Foxq1*$^{-/-}$ pups appear normal at birth and develop a silky coat. Analysis of gastric physiology in the mutant animals demonstrates that FOXQ1 is required for the function of the acid secretory system. These variable phenotypes provide evidence for multiple roles of FOXQ1 during embryogenesis and adult life.

Materials and methods

Generation of Foxq1-deficient mice

A lambda phage clone carrying the complete *Foxq1* gene was isolated from a 129/Sv genomic mouse library (Frank and Zoll, 1998). The genomic clone was characterised by restriction enzyme mapping and sequencing. The 10-kb *Not*I-*Xho*I and 2.5-kb *Sst*1 genomic fragments were subcloned into the QuanTox vector (Qbiogene). The 2.5-kb *Sst*I fragment containing the 3′-flanking region was isolated and ligated with *Xba*I/*Eco*RI-digested pPNT vector (Tybulewicz et al., 1991) after treating with Klenow enzyme (clone Foxq1/1). The 10-kb *Not*I-*Xho*I fragment was used as a 5′-flanking region and inserted into the *Not*I-*Xho*I restricted clone Foxq1/1. The resulting targeting vector (Fig. 2A) was linearized with *Not*I and transfected into RI embryonic stem (ES) cells, and clones resistant to G418 (400 μg/ml) and 2 μM ganciclovir were isolated (Wurst and Joyner, 1993). Genomic DNA extracted from drug-resistant ES-clones was digested with *Bam*HI, electrophoresed and blotted onto nitrocellulose membrane. The 453-bp *Sst*I fragment located externally 3′ of the targeting vector was radioactively labelled and used to probe the Southern blots. Hybridization was carried out at 65°C overnight in RapidHyb buffer (Amersham Bioscience) following the manufacturer's protocol. Filters were washed twice at 65°C at a final stringency of 0.2× SSC, 0.1% SDS. Cells from two recombinant ES clones were injected into C57BL/6J blastocysts, and these were transferred into DBA/BL6 pseudopregnant females. Germ line-transmitting chimeric males obtained from both lines were backcrossed to C57BL/6J and 129/Sv females.

To genotype the mice, genomic DNA was extracted from tails and analyzed by PCR. Thermal cycling was carried out for 35 cycles with denaturation at 94°C for 30 s, annealing at 58°C for 45 s and extension at 72°C for 1 min. The following primers were used to discriminate wild-type and mutant alleles: primer F1: 5′-CACCTGTACTGCCCCCTACG-3′, and primer R1: 5′-TGGACTAAGTTAAAACACTTGGGTCA-3′ were designed to amplify wild-type loci. The primer N1: 5′-CCTTCTATCGCCTTCTTGACG-3′ was designed to amplify the targeted locus (Fig. 2A). A 299-bp fragment of the wild type allele was amplified with primers F1 and R1, whereas primers N1 and R1 amplified a 575-bp fragment of the mutant allele.

All animal experiments were reviewed and approved by the Institutional Animal Care and Use Committee of the University of Göttingen.

Northern blots and RT-PCR

Total RNA was extracted from tissues using a QIAGEN RNA kit (QIAGEN, Germany) according to the manufacturer's instructions. To determine gene expression in stomach, the stomachs were removed from adult mice that had been fasted overnight. For Northern blot analysis, 20 μg of RNA was electrophoresed in 1.5% agarose gels containing 2.2 M formaldehyde, transferred to nitrocellulose membranes (Amersham Bioscience) and hybridized with ^{32}P-labeled probe at the same conditions as used for Southern blot hybridization.

For semi-quantitative RT-PCR analysis, total RNA (2 μg) was reverse transcribed into cDNA at 42°C for 50 min using a poly (dT)-oligonucleotide and the Superscript Reverse Transcriptase kit (Invitrogen). One microliter of the cDNA was then subjected to 35 cycles of PCR. Aliquots of amplified products were taken after the PCR-cycles 28, 30, 32 and 35, and analyzed in 1.5% agarose gels. Primer sequences to amplify cholecystokinine receptor (*Cckbr; Sos2*), histamine H2 receptor (*Hrh2*), ezrin (*Vil2*), telokin (*Mylk*) and *Hprt* were 5′-GATGGTGATAATGACAGCGAGA-3′ and 5′-AGGTGTAGCTCAGCAAGTGGAT-3, 5′-TCCTCACCACCCTCATCTTC-3′ and 5′-ATCCCATCCACCAGTCCATA-3′, 5′-CGAGAAGAAGAGGCGAGAGA-3′ and 5′-TGTAGCCCATAGGCTCTGCT-3′, 5′-CGAGAACATCATGTGTGTCAAC-3′ and 5′-CCATGTTCTTGGTGTCTTTCAT-3′, and 5′-CGTCGTGATTAGCGATGATG-3′ and 5′-TATGTCCCCCGTTGACTGAT-3′, respectively.

Measurements of gastric pH and output of acid-base equivalents

A measurement of gastric acid output was performed by modification of the method described by Wood and Dubois (1983). Briefly, 3-month-old mice were fasted overnight with free access to water. Each mouse was injected intraperitoneally with a sterile solution of histamine HCl (10 μg/g body weight, Sigma) or pentagastrin (1μg/g body weight, Sigma) in 0.9% NaCl solution. At different time points after injection, mice were sacrificed and the abdomen was immediately opened. After clamping the gastroesophageal and pyloric junctions, the stomach was then immersed in 2 ml oxygen-saturated normal saline solution and opened along the greater curvature to release the gastric contents. The stomach was then removed, blotted dry with absorbent paper, and weighed. The gastric content was centrifuged at 500 *g* for 5 min, and the supernatant was used for measuring the pH value. After determination of the pH, the supernatant was titrated with 0.01 N NaOH or 0.01 N HCl. Results are expressed as microequivalents of H^+ or OH^- per gram of stomach wet weight.

Biochemical analysis of blood

Trunk blood was collected into heparinised tubes for analysis on an AVL OMN19 (Roche, Mannheim, Germany) blood gas analyzer.

Histological analysis, immunohistochemistry and in situ hybridization

Embryos were collected in PBS, fixed in Bouin's fixative, embedded in paraffin, sectioned, and stained with hematoxylin-eosin. Stomachs were opened and washed three times in PBS to remove stomach content. Stomachs were fixed in Bouin's fixative or pinned on cork and fixed in 4% paraformaldehyde. After embedding in paraffin, and sectioning at 5–7 μm, Bouin's fixed sections were used for hematoxylin-eosin staining. Paraformaldehyde-fixed sections were subjected to immunohistochemical analysis and in situ hybridization.

For immunohistochemistry, paraformaldhyde fixed sections were preincubated for 1 h with 5% normal goat serum in 0.05% Triton X-100/PBS and incubated overnight at 4°C with the primary antibodies, washed three times in PBS and incubated for 1 h with secondary antibodies, washed three times with PBS, and then stained with DAPI (4′,6-diamidino-2-phenylindole; Vector). Slides were examined with a BX60 microscope (Olympus, Hamburg, Germany) with fluorescence equipment and analysis software program (Soft Imaging System, Münster, Germany). Monoclonal anti-H^+, K^+-ATPase β-subunit was diluted at 1:1000 (Acris Antibodies, Hiddenhausen, Germany). Secondary antibodies were goat anti-mouse fluorescein isothiocyanate (Sigma).

The digoxigenin-UTP-labeled riboprobes were synthesized using the DIG RNA labeling Kit (Roche, Germany) from linearized plasmid templates containing the 5′ region of *Foxq1* cDNA. Antisense and sense RNA probes were then used to hybridize the stomach sections. Prehybridization, hybridization and washing was performed according to the manufacturer's manual of DIG Nucleic Acid Detection Kit (Roche). Slides were imaged as described above.

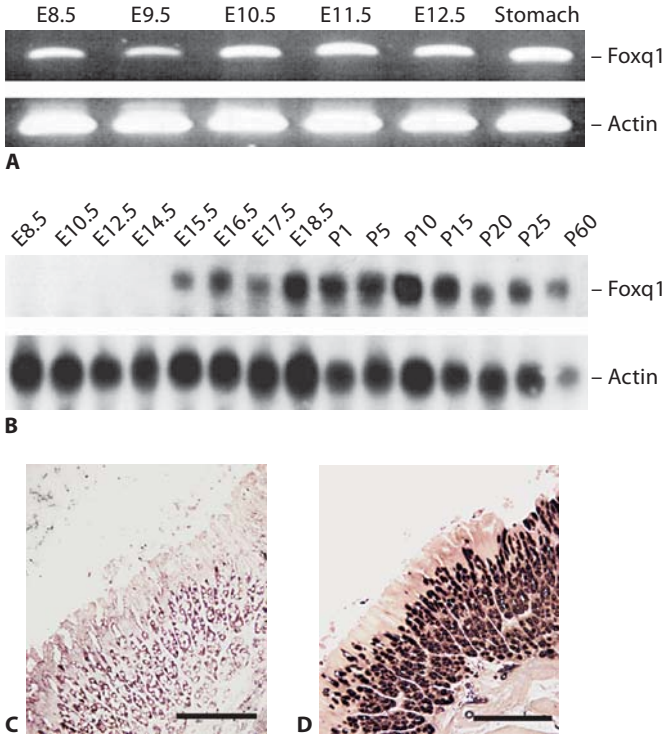

Fig. 1. Expression analyses of the *Foxq1* gene. (**A**) RT-PCR analysis with total RNA and *Foxq1* specific primers showed the presence of a 265-bp amplified product in all examined embryonic stages (E8.5–E12.5). (**B**) Northern blot with total RNA from whole embryos (E8.5–E14.5), and from stomach of E15.5–E18.5 and different postnatal days (P1–P60). Hybridization of blot with *Foxq1* cDNA showed high expression of Foxq1 in the stomach of E15.5 and the expression levels maintain equivalent through neonatal stages and adulthood. Rehybridization of the blot with *β-actin* probe revealed the integrity of RNA loading. (**C**) In situ hybridization of DIG-labelled *Foxq1* antisense to wild-type stomach sections. (**D**) An equivalent section was immunostained with anti-H^+,K^+-ATPase β-subunit antibody. Scale bars: panels **C** and **D**, 100 μm.

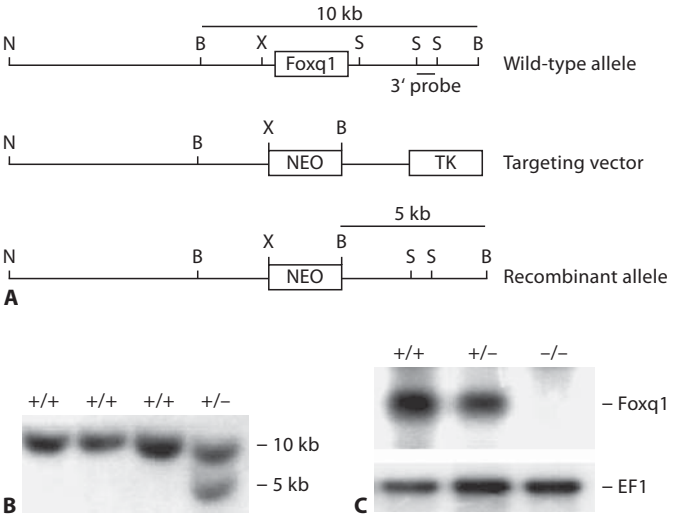

Fig. 2. Targeted disruption of the *Foxq1* gene. (**A**) The structures of the wild-type allele, the targeting vector, and recombinant allele are shown together with the relevant restriction sites. A 2-kb *Xho*I-*Sst*I fragment containing the whole coding region of *Foxq1* was replaced by a *pgk-neo* selection cassette (NEO). The 3′ external probe used and the predicted length of *Bam*HI restriction fragments in Southern blot analysis are shown. Abbreviations: TK, *Thymidine kinase* cassette; N, *Not*I; B, *Bam*HI; X, *Xho*I; S, *Sst*I; K, *Kpn*I. (**B**) Southern blot analysis of recombinant ES cell clones. Genomic DNA extracted from ES cell clones was restricted with *Bam*HI and probed with the 3′ probe shown in panel **A**. The wild-type allele generated a 10-kb *Bam*HI fragment, whereas the targeted allele yielded a 5-kb *Bam*HI fragment, as indicated in panel **A**. (**C**) Northern blot analysis with total RNA isolated from stomach of $Foxq1^{+/+}$, $Foxq1^{+/-}$ and $Foxq1^{-/-}$ adult mice was hybridized with a *Foxq1*-specific cDNA probe. Rehybridization of blot with human elongation factor-1 (EF1) revealed the integrity of RNA loading.

Electron microscopy

Mice were injected with pentagastrin as described above. After 60 min of gastrin treatment the stomach was dissected and fixed in freshly prepared 1.5% paraformaldehyde, 1.5% glutaraldehyde in 0.15 M HEPES buffer. Tissue blocks were osmicated, stained in 1.5% aqueous uranyl acetate overnight, dehydrated in acetone, and finally embedded in longitudinal and transversal orientation in araldite as described previously (Fehrenbach and Ochs, 1998).

Results

Foxq1 is expressed in the parietal cells of gastric mucosa

Expression analyses of *Foxq1* in adult mouse tissues revealed that *Foxq1* is highly expressed in the stomach (Frank and Zoll, 1998). To evaluate the expression of *Foxq1* during prenatal development and stomach maturation, we performed RT-PCR and Northern blot analyses. As shown in Fig. 1A, *Foxq1* transcripts were detected by RT-PCR at different stages (from embryonic days 8.5 to 12.5). Northern blot analysis showed a high expression of *Foxq1* in the stomach at embryonic day 15.5 and the expression levels were maintained through neonatal stages and adulthood (Fig. 1B). To ascertain whether a specific compartment of the stomach shows high expression of *Foxq1*, in situ hybridization was undertaken on sections of adult stomach. The antisense *Foxq1* probe hybridized with cells located in the glandular epithelium (Fig. 1C). Immunohistochemical staining of equivalent serial sections with antibodies to the H^+,K^+-ATPase β-subunit, which is a marker for parietal cells, revealed that the expression of *Foxq1* in stomach is restricted to parietal cells (Fig. 1D).

Targeted disruption of Foxq1

To investigate the physiological function of *Foxq1* in the mouse, we generated *Foxq1*-deficient mice by gene targeting. A *Foxq1* targeting construct was designed to replace a 2.0-kb genomic fragment containing the entire coding region of *Foxq1* by the neomycin resistance gene (neo^r) (Fig. 2A). ES cells were transfected with the targeting vector and selected for homologous recombination. Drug-resistant clones were selected, and DNA was screened by Southern blot analysis with a 3′ external probe. The external probe

detected a 10-kb *Bam*HI wild-type fragment and a 5-kb *Bam*HI recombinant fragment (Fig. 2A and B). Two *Foxq1*$^{+/-}$ ES cell lines with a correctly targeted allele were identified and cells were injected in C57BL/6J blastocysts. The resulting male chimeras were crossed with C57BL/6J or 129/Sv females to establish the *Foxq1*-disrupted allele on a C57BL/6J × 129/Sv hybrid and on a 129/Sv inbred genetic background. Both ES cell lines transmitted the mutation into the germline. The heterozygous animals appeared normal and were intercrossed to obtain homozygous null animals. *Foxq1*$^{-/-}$ animals exhibited normal growth and survival compared with wild-type littermates. Both male and female *Foxq1*$^{-/-}$ mice were fertile. However, *Foxq1*$^{-/-}$ mice display satin hair similar to satin mutant mice, which have a spontaneous mutation in the *Foxq1* locus (Hong et al., 2001).

To confirm the inactivation of *Foxq1* we performed Northern blot analyses. Total RNA from stomach tissues was isolated from 3-month-old wild-type, *Foxq1*$^{+/-}$ and *Foxq1*$^{-/-}$ mice. Northern blot analysis failed to detect *Foxq1* mRNA in the *Foxq1*$^{-/-}$ stomach (Fig. 2C).

Foxq1-deficient mice exhibit increased embryonic lethality

Expression of *Foxq1* in early embryonic development led us to determine the consequence of *Foxq1* deficiency for embryonic development. A total of 191 F2 live-born progeny at three weeks was genotyped and we found 31.7% *Foxq1*$^{+/+}$, 53.3% *Foxq1*$^{+/-}$ and 15.0% *Foxq1*$^{-/-}$ mice. Litter size of *Foxq1*$^{-/-}$ intercrosses was significantly smaller (average litter size, 4.5 ± 2.2 [n = 15]; average wild-type litter size, 9.1 ± 1.3 [n = 15]). These results prompted us to determine the embryonic stage where the reduction of *Foxq1*$^{-/-}$ embryos occurs. Embryos from timed wild-type and *Foxq1*$^{-/-}$ mating were analysed at different days of gestation (Fig. 3A). At E8.5, no deviation in the number of embryos was observed between these groups. At E10.5, the number of *Foxq1*$^{-/-}$ embryos decreased to approximately 85%, dropped to 69% at E12.5 and 44% at E15.5. The wild-type control group exhibits a decrease of approximately 6% between E8.5 and E15.5. Morphological examinations revealed that around 50% of *Foxq1*-deficient embryos at E10.5 display head abnormalities. Head malformation was characterized by shrinkage of the brain vesicle possibly due to reduced cerebrospinal fluid volume (Fig. 3D and E). However, normal developed *Foxq1*$^{-/-}$embryos did not differ histologically from wild-type littermates (Fig. 3B and C). No head malformation was observed in *Foxq1*-deficient embryos at E12.5. However, a notable number of resorbed embryos were recovered from litters examined at E12.5 indicating the lethality of malformed *Foxq1*$^{-/-}$ embryos between E10.5 and E12.5. In all examined *Foxq1*$^{-/-}$ embryos, we observed normal organogenesis of fetal liver, heart and extraembryonic placenta tissue when compared with *Foxq1*$^{+/+}$ and *Foxq1*$^{+/-}$ littermates (data not shown). Therefore, the exact cause of embryonic lethality, although undetermined, cannot be attributed to a placental defect. The observed embryonic lethality of *Foxq1*$^{-/-}$ is restricted to the C57BL/6J × 129/Sv mixed genetic background.

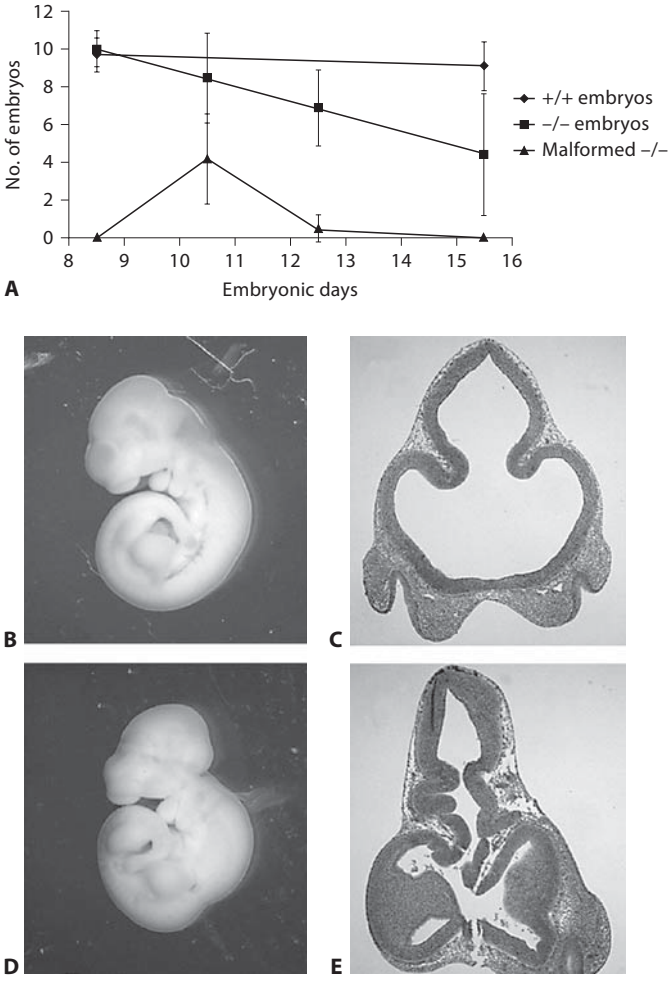

Fig. 3. *Foxq1*$^{-/-}$ mice exhibit embryonic lethality on C57BL6/6J × 129/Sv hybrid background. (**A**) Number of embryos derived from wild-type and *Foxq1*$^{-/-}$ intercrosses was counted for each embryonic stage. The number of malformed embryos derived from *Foxq1*$^{-/-}$ intercrosses was also counted. Each value represents mean ± standard deviation of the results from 10 litters for each intercross. (**B**, **D**) Micrographs of E10.5 embryos derived from wild-type (**B**) and *Foxq1*$^{-/-}$ (**D**) matings. (**C**, **E**) Hematoxylin-eosin staining of transverse sections through the forebrain shows shrinkage of the third and lateral ventricles (**E**).

Loss of acid secretion in Foxq1-deficient mice

Histological analysis was performed with adult kidney and stomach, in which *Foxq1* is predominantly expressed. Despite the high levels of *Foxq1* in both tissues, no significant histopathology was observed in these tissues of *Foxq1*-null mice (Fig. 4A and B, and data not shown).

To determine whether the absence of *Foxq1* in kidney might cause disturbance of acid-base or ion homeostasis, we analysed blood gases, pH and electrolyte concentration under normal conditions. Blood pH, HCO_3, and Na^+, Ca^+ and K^+ concentration were virtually identical in both groups of wild-type and *Foxq1*-null mice (data not shown) indicating that the lack of *Foxq1* caused no significant perturbation of acid-base or ion homeostasis.

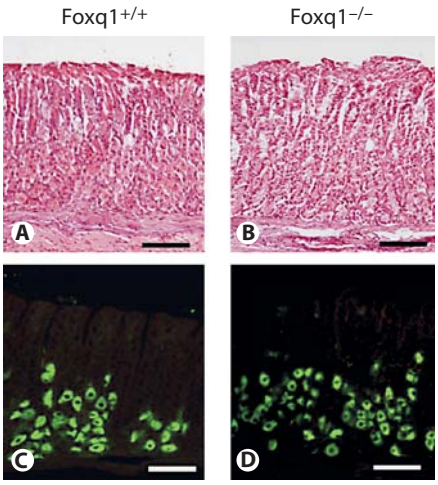

Fig. 4. Histological comparison of the gastric mucosa in the fundic region of wild-type (**A**, **C**) and Foxq1-deficient mice (**B**, **D**). (**A**, **B**) Hematoxylin-eosin stained sections demonstrate that the overall morphology is not markedly different in Foxq1-deficient mice. Immunohistochemical staining of parietal cells with anti-H^+,K^+-ATPase β-subunit (**C**, **D**) demonstrated no marked changes in number of parietal cells per gastric gland in wild-type and *Foxq1*$^{-/-}$ stomach. Scale bars: panels **A** and **B**, 100 μm; panels **C** and **D**, 200 μm.

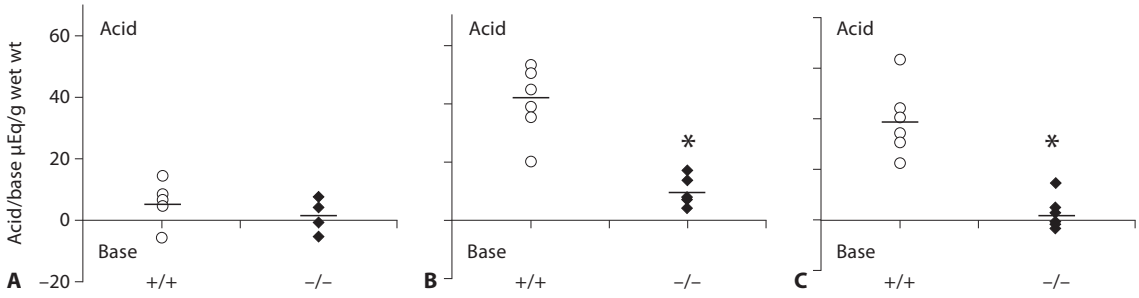

Fig. 5. Gastric acid secretion in wild-type (open circles) and Foxq1-deficient (filled diamonds) mice. (**A**) Basal gastric acid output. Acid secretion was stimulated by intraperitoneal injection of histamine and gastrin. Acid output was determined after 30 and 60 min of histamine (**B**) and gastrin (**C**) stimulation, respectively. Horizontal bars represent mean values of data for each genotype. Asterisk denotes statistically significant difference from wild-type mice by t test ($P < 0.0001$). There was no significant difference in values of basal acid output between wild-type and Foxq1-deficient mice ($n = 6$ mice/group). Total acid and base equivalents were determined by titration with either 0.01 N NaOH or HCl. Data were normalized to the blotted wet weight (wet wt) of the stomach.

To determine the consequence of *Foxq1* deficiency on the development of parietal cells, we performed immunohistochemistry using a parietal specific marker, H^+/K^+-ATPase β-subunit (Fig. 4C and D). Cell counts of H^+/K^+-ATPase β-subunit expressing cells per gastric unit of *Foxq1*$^{+/+}$ and *Foxq1*$^{-/-}$ mice showed the presence of roughly equivalent numbers of parietal cells in the wild-type (12.8 ± 1.9) and *Foxq1*-deficient (12.0 ± 1.5) mice ($P > 0.05$; n = 50 glands). This result indicates that the *Foxq1* deficiency does not impair the development of parietal cells.

The specific expression of *Foxq1* in the parietal cells, which are the acid secreting cells within the stomach, prompted us to assume a role of Foxq1 in the regulation of gastric acid secretion. We first measured intragastric pH in overnight fasted mice. The basal gastric pH in *Foxq1*-null mice was not significantly different from that in wild-type mice (6.79 ± 0.22 vs. 6.97 ± 0.18: $P > 0.05$) (Fig. 5A). Acid secretion was then measured at different time points after administration of histamine and gastrin, and found that gastric acid secretion is highly stimulated in wild-type stomach after 30 and 60 min of histamine and gastrin treatment, respectively (data not shown). In stomach of *Foxq1*$^{-/-}$ mice, acid secretion was undetectable and there was no response to stimulation with histamine or gastrin. In contrast, the acid output induced by histamine and gastrin was increased approximately sevenfold in wild-type mice (40.5 ± 10.9 μEq/g and 39.4 ± 12.9 μEq/g, respectively), as compared to basal level (5.8 ± 5.9 μEq/g) (Fig. 5B and C).

Expression analysis of genes regulating gastric acid secretion

We examined the consequence of *Foxq1* deficiency on the expression of several genes, whose inactivation in mice affects gastric acid secretion. Northern blot analysis did not show significant difference in the expression of gastrin (*Gast*) and H, K ATPase α-subunit (*Atpa4a*) in *Foxq1*$^{+/+}$ and *Foxq1*$^{-/-}$ stomach, whereas the expression of somatostatin was significantly reduced in *Foxq1*$^{-/-}$ stomach (Fig. 6A). A decreased expression of somatostatin mRNA in stomach

was not observed in pancreas of *Foxq1*$^{-/-}$ (data not shown). In addition, semi-quantitative RT-PCR analysis of histamine H2-receptor (*Hrh2*), gastrin-receptor (*Cckbr*), ezrin (*Vil2*) expression did not exhibit marked differences between wild-type and mutant mice (Fig. 6B). Hoggatt et al. (2000) reported that *Foxq1* regulates the expression of the smooth muscle protein telokin (*Mylk*). However, RNA analysis did not show a distinct alteration in *Mylk* expression in *Foxq1*$^{-/-}$ stomach (Fig. 6B).

Defects in the formation/expansion of apical secretory canaliculi in Foxq1$^{-/-}$ *parietal cells*

We investigated whether the defects in gastric acid secretion can be correlated with ultrastructural alteration of *Foxq1*$^{-/-}$ parietal cells in resting state and upon secretagogue stimuli. *Foxq1*$^{+/+}$ and *Foxq1*$^{-/-}$ mice were fasted in order to suppress the secretion of gastric juice. In wild-type and Foxq1-deficient parietal cells, secretory canaliculi with numerous microvilli were readily observed. Tubulovesicles, which are similar in dimension and appearance to canalicular microvilli, were densely located just beneath the canalicular membrane (Fig. 7A and B). To determine the effect of secretagogue stimuli on parietal cells, mice were fasted overnight, and stomachs were collected for fixation 60 min after gastrin treatment. Measurements of pH of gastric juice from wild-type stomach indicated that the drug treatments were effective (data not shown). In gastrin-stimulated wild-type parietal cells, the luminal space of the secretory canaliculi was markedly expanded and tubulovesicles were decreased in number due to a fusion of cytoplasmic tubulovesicular structures to the apical canalicular plasma membrane (Fig. 7C). In contrast, most of *Foxq1*$^{-/-}$ parietal cells showed the morphological appearance of resting cells. The gastrin-treatment did not induce the expansion of apical secretory canaliculi, leaving the cytoplasm densely packed with tubulovesicles (Fig. 7D). These results indicate that *Foxq1*$^{-/-}$ parietal cells were less responsive to gastrin, and that this might be the main cause for the impairment of gastric secretion.

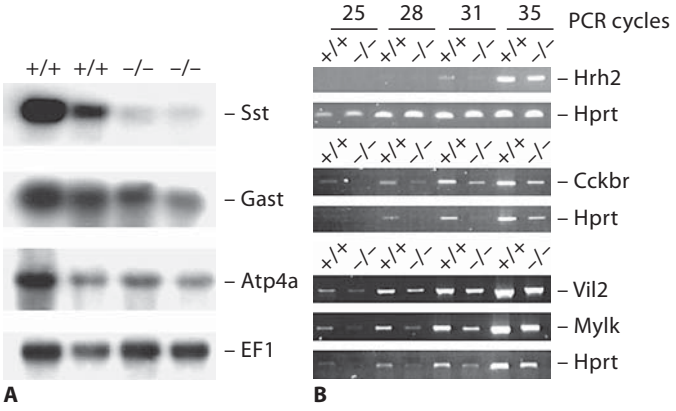

Fig. 6. Expression analysis of genes regulating the gastric acid secretion. (**A**) Total RNA was isolated from stomachs of 8-week-old *Foxq1*$^{+/+}$ and *Foxq1*$^{-/-}$ mice. Blot was hybridized sequentially with probes to somatostatin (*Sst*), gastrin (*Gast*) and H^+,K^+-ATPase α-subunit (*Atp4a*) and human elongation factor-1 (EF1) as a loading control. (**B**) Semi-quantative RT-PCR assays were performed to determine the expression levels of gastrin receptor (*Cckbr*), histamine H2 receptor (*Hrh2*), ezrin (*Vil2*), and telokin (*Mylk*) gene in stomach of wild-type and FOXQ1-deficient mice.

Discussion

The goal of this study was to determine the role of the transcription factor FOXQ1 in development and function of parietal cells. This study was motivated by the strong, selective expression of *Foxq1* in gastric parietal cells of mouse. The expression of *Foxq1* in stomach is evolutionarily conserved. Thus, it has been found that *Foxq1* is expressed in stomach of *Xenopus* during prenatal development (Choi et al., 2006).

Analyses of *Foxq1*-null mice showed that the Foxq1 deficiency does not impair the differentiation and maintenance of parietal cells, but severely affects the parietal cell function. Basal gastric secretion was abolished and could not be induced by the major acid secretagogues including histamine or gastrin. Expression of gastrin, gastrin-, histamine H2-receptor and H^+,K^+-ATPase α subunit gene, which play a role in acid secretion (Samuelson and Hinkle, 2003), in stomach of wild-type and *Foxq1*$^{-/-}$ mice did not reveal any obvious change suggesting that FOXQ1 does not regulate these genes. Reduced expression of somatostatin in *Foxq1*$^{-/-}$ stomach might be not the result of FOXQ1-deficiency in the parietal cells, but could be attributed to reduced acid secretion, which normally exerts an inhibitory effect on the expression of somatostatin in the D-cells (Holst et al., 1992; Pashankar et al., 2001; Yip et al., 2004).

Parietal cells in resting state contain a large amount of tubulovesicles. Upon stimulation of parietal cells to secrete acid, this tubulovesicular membrane is incorporated into the apical plasma membrane to expand the secretory canaliculi. Tubulovesicles are reformed by entocytic retrieval from canalicular membrane as the cell returns to the resting state (Agnew et al., 1999; Yao and Forte, 2003). Ultrastructural data presented here demonstrate that the tubulovesicles are largely abundant in the *Foxq1*$^{-/-}$ parietal cells, while the secretory canaliculi are not expanded in gastrin-stimulated *Foxq1*$^{-/-}$ parietal cells. These results suggest that the FOXQ1-regulated genes are not required for genesis of the tubulovesicular compartments, but are necessary for the formation/expansion of canalicular apical membranes in gastric parietal cells.

Various knockout mouse models have shown altered gastric secretory capabilities (Friis-Hansen et al., 1998; Schultheis et al., 1998; Aihara et al., 1999; Kobayashi et al., 2000; Spicer et al., 2000; Gawenis et al., 2004, 2005; Kato et al., 2004; Roepke et al., 2006). The underlying causes for impaired acid secretion in these mutant strains are different. The failure of tubulovesicular membranes to fuse with the apical membranes of canaliculi in *Foxq1*$^{-/-}$ parietal cells is similar to that seen in ezrin knockdown mice (Tamura et

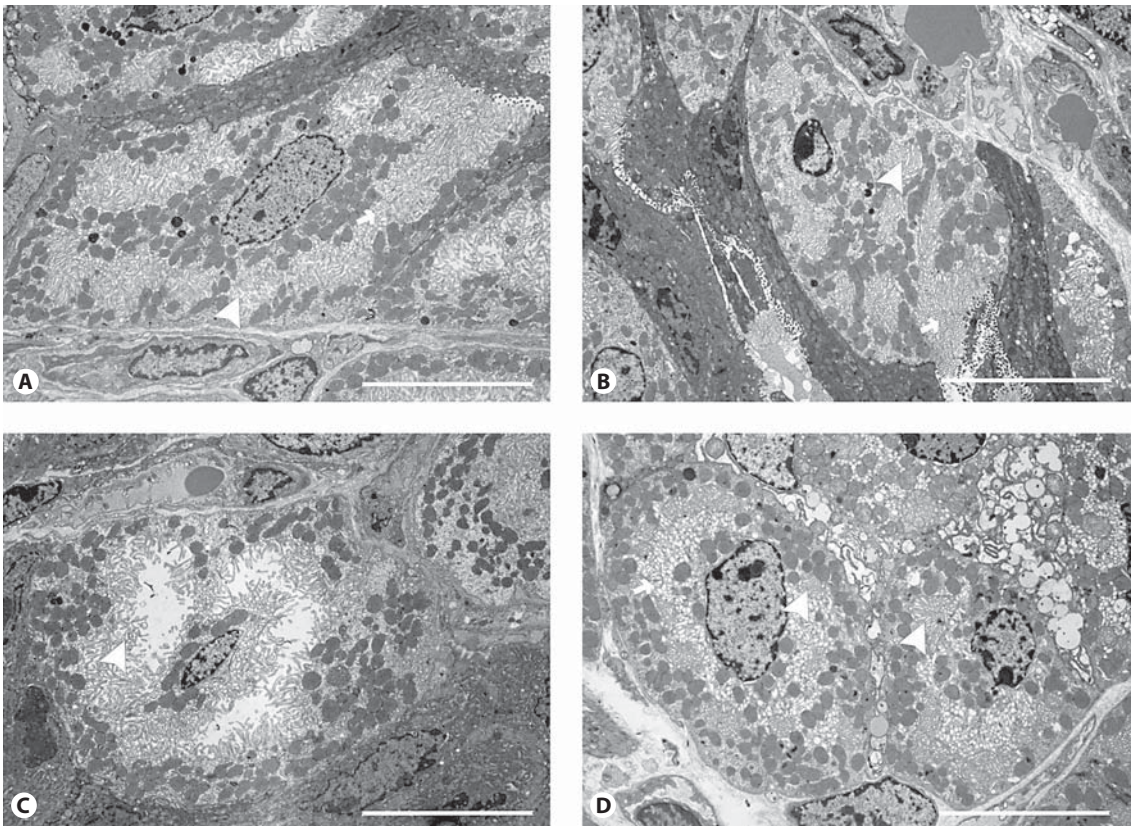

Fig. 7. Electron micrographs of parietal cells from fasted wild-type (**A**) and *Foxq1*$^{-/-}$ (**B**) showed typical secretory canaliculi (arrowhead) with numerous tubulovesicles (arrow). (**C**, **D**) Ultrastructure of parietal cells after gastrin stimulation. Wild-type parietal cells contain massively extended apical membrane of secretory canaliculi (arrowhead) and relatively few tubulovesicles (arrow) in the cytoplasm (**C**). In contrast, most of Foxq1-deficient parietal cells appeared in the resting state, characterized by narrow secretory canaliculi and numerous tubulovesicles in the cytoplasm (**D**). Scale bars: 10 μm.

al., 2005). The cytoskeleton-associated protein ezrin, a member of the ezrin/radixin/moesin (ERM) family, is believed to be one of the critical participants in membrane folding and the modulation of secretory membranes (Forte et al., 1998). Defects in the expansion of apical secretory canaliculi in Foxq1- and ezrin-deficient parietal cells lead us to suggest that Foxq1 might regulate the expression of the ezrin gene. However, the ezrin gene was not found to be downregulated in the stomach of Foxq1-deficient mice. Furthermore, Foxq1 has been found to mediate repressing effects in the regulation of smooth muscle specific genes *Mylk, SM22α* and *γ-actin* in nonmuscle cells (Hoggatt et al., 2000). However, RNA analysis did not reveal an alteration in *Mylk* expression in *Foxq1*$^{-/-}$ stomach.

We have further observed several striking morphological anomalies associated with Foxq1 deficiency. In the hybrid genetic background, 50% of *Foxq1*$^{-/-}$ embryos die in utero at about 10.5 to 12.5 days p.c. and display head abnormalities. However, the incidence of embryonic lethality of *Foxq1*$^{-/-}$ is lower in the inbred 129/Sv background, presumably due to the effect of different combinations of modifier genes. In contrast, the satin hair phenotype is fully penetrant with Foxq1 deficiency in both genetic backgrounds.

On the basis of *Foxq1* expression in mouse kidney (Frank and Zoll, 1998), it seems possible that FOXQ1 might play a role in regulation of kidney development and/or function. However, we observed no physiological perturbations that could be attributed to altered renal function. There were no apparent differences in blood pH, HCO_3 and Na^+ levels between *Foxq1*$^{-/-}$ and *Foxq1*$^{+/+}$ mice.

In summary, our results suggest that Foxq1 plays a crucial role in the formation/expansion of canalicular apical membranes in gastric parietal cells, leading to gastric acid secretion. Therefore, *FOXQ1* may be added to the growing list of candidate genes that causes achlorhydria in human.

Acknowledgments

We thank M. Schindler, H. Riedesel and S. Wolf for help in the generation and breeding of knockout mice.

References

Agnew BJ, Duman JG, Watson CL, Coling DE, Forte JG: Cytological transformations associated with parietal cell stimulation: critical steps in the activation cascade. J Cell Sci 112:2639–2646 (1999).

Aihara T, Fujishita T, Kanatani K, Furutani K, Nakamura E, et al: Impaired gastric secretion and lack of trophic responses to hypergastrinemia in M3 muscarinic receptor knockout mice. Gastroenterology 125:1774–1784 (1999).

Champagne ET: Low gastric hydrochloric acid secretion and mineral bioavailability. Adv Exp Med Biol 249:173–184 (1989).

Chew CS: Parietal cell protein kinases. Selective activation of type I cAMP-dependent protein kinase by histamine. J Biol Chem 260:7540–7550 (1985).

Choi VM, Harland RM, Khokha MK: Developmental expression of FoxJ1.2, FoxJ2, and FoxQ1 in *Xenopus tropicalis*. Gene Expr Patterns 6:443–447 (2006).

Clark KL, Halay ED, Lai E, Burley SK: Co-crystal structure of the HNF-3/fork head DNA-recognition motif resembles histone H5. Nature 364:412–420 (1993).

Fehrenbach H, Ochs M: Studying lung ultrastructure, in Uhlig S, Taylor AE (eds): Methods in Pulmonary Research, pp 429–456 (Birkhäuser Publishers, Basel 1998).

Forte JG, Ly B, Rong Q, Ogihara S, Ramilo M, et al: State of actin in gastric parietal cells. Am J Physiol 274:C97–104 (1998).

Frank S, Zoll B: Mouse HNF-3/fork head homolog-1-like gene: structure, chromosomal location, and expression in adult and embryonic kidney. DNA Cell Biol 17:679–688 (1998).

Friis-Hansen L, Sundler F, Li Y, Gillespie PJ, Saunders TL, et al: Impaired gastric acid secretion in gastrin-deficient mice. Am J Physiol 274:G561–568 (1998).

Fukushima Y, Ohmachi Y, Asano T, Nawano M, Funaki M, et al: Localization of the histamine H2 receptor, a target for antiulcer drugs, in gastric parietal cells. Digestion 60:522–527 (1999).

Gawenis LR, Ledoussal C, Judd LM, Prasad V, Alper SL, et al: Mice with a targeted disruption of the AE2 Cl-/HCO3- exchanger are achlorhydric. J Biol Chem 279:30531–30539 (2004).

Gawenis LR, Greeb JM, Prasad V, Grisham C, Sanford LP, et al: Impaired gastric acid secretion in mice with a targeted disruption of the NHE4 Na+/H+ exchanger. J Biol Chem 280:12781–12789 (2005).

Hoggatt AM, Kriegel AM, Smith AF, Herring BP: Hepatocyte nuclear factor-3 homologue 1 (HFH-1) represses transcription of smooth muscle-specific genes. J Biol Chem 275:31162–31170 (2000).

Holst JJ, Orskov C, Seier-Poulsen S: Somatostatin is an essential paracrine link in acid inhibition of gastrin secretion. Digestion 51:95–102 (1992).

Hong HK, Noveroske JK, Headon DJ, Liu T, Sy MS, et al: The winged helix/forkhead transcription factor Foxq1 regulates differentiation of hair in satin mice. Genesis 29:163–171 (2001).

Kaestner KH, Knochel W, Martinez DE: Unified nomenclature for the winged helix/forkhead transcription factors. Genes Dev 14:142–146 (2000).

Kato Y, Fukamachi H, Takano-Maruyama M, Aoe T, Murahashi Y, et al: Reduction of SNAP25 in acid secretion defect of *Foxl1*–/– gastric parietal cells. Biochem Biophys Res Commun 320:766–772 (2004).

Kaufmann E, Knochel W: Five years on the wings of fork head. Mech Dev 57:3–20 (1996).

Kobayashi T, Tonai S, Ishihara Y, Koga R, Okabe S, et al: Abnormal functional and morphological regulation of the gastric mucosa in histamine H2 receptor-deficient mice. J Clin Invest 105:1741–1749 (2000).

Pashankar DS, Israel DM, Jevon GP, Buchan AM: Effect of long-term omeprazole treatment on antral G and D cells in children. J Pediatr Gastroenterol Nutr 33:537–542 (2001).

Roepke TK, Anantharam A, Kirchhoff P, Busque SM, Young JB, et al: The KCNE2 potassium channel ancillary subunit is essential for gastric acid secretion. J Biol Chem 281:23740–23747 (2006).

Samuelson LC, Hinkle KL: Insights into the regulation of gastric acid secretion through analysis of genetically engineered mice. Annu Rev Physiol 65:383–400 (2003).

Schultheis PJ, Clarke LL, Meneton P, Harline M, Boivin GP, et al: Targeted disruption of the murine Na+/H+ exchanger isoform 2 gene causes reduced viability of gastric parietal cells and loss of net acid secretion. J Clin Invest 101:1243–1253 (1998).

Spicer Z, Miller ML, Andringa A, Riddle TM, Duffy JJ, et al: Stomachs of mice lacking the gastric H, K-ATPase alpha-subunit have achlorhydria, abnormal parietal cells, and ciliated metaplasia. J Biol Chem 275:21555–21565 (2000).

Tamura A, Kikuchi S, Hata M, Katsuno T, Matsui T, et al: Achlorhydria by ezrin knockdown: defects in the formation/expansion of apical canaliculi in gastric parietal cells. J Cell Biol 169:21–28 (2005).

Tybulewicz VL, Crawford CE, Jackson PK, Bronson RT, Mulligan RC: Neonatal lethality and lymphopenia in mice with a homozygous disruption of the c-abl proto-oncogene. Cell 65:1153–1163 (1991).

Urushidani T, Forte JG: Signal transduction and activation of acid secretion in the parietal cell. J Membr Biol 159:99–111 (1997).

Wood LR, Dubois A: Scanning electron microscopy of the stomach during modifications of acid secretion. Am J Physiol 244:G475–479 (1983).

Wurst W, Joyner AL: Production of targeted embryonic stem cell clones, in Joyner AL (ed): Gene Targeting: a Practical Approach, pp 33–61 (IRL Press, Oxford 1993).

Yao X, Forte JG: Cell biology of acid secretion by the parietal cell. Annu Rev Physiol 65:103–131 (2003).

Yip L, Leung HC, Kwok YN: Effect of omeprazole on gastric adenosine A1 and A2A receptor gene expression and function. J Pharmacol Exp Ther 311:180–189 (2004).